European Review for Medical and Pharmacological Sciences 2019; 23: 9642-9650

Effects of butylphthalide on oxidative stress and inflammatory response in rats with myocardial infarction through Akt/Nrf2 signaling pathway

M. BAI[1,2,3,4], C.-L. PAN[1,2,3,4], G.-X. JIANG[1,2,3,4], Y.-M. ZHANG[1,2,3,4], Z. ZHANG[1,2,3,4]

[1]Department of Cardiology, The First Hospital of Lanzhou University, Lanzhou, China
[2]Gansu Provincial Clinical Research Center for Cardiovascular Diseases, Lanzhou, China
[3]Gansu Provincial Key Laboratory of Cardiovascular Disease, Lanzhou, China
[4]National Project of Improving the Diagnosis and Treatment Ability of Cardiovascular and Cerebrovascular Diseases, The First Hospital of Lanzhou University, Lanzhou, China

Abstract. – OBJECTIVE: The aim of this study was to investigate the effects of butylphthalide on oxidative stress and inflammatory response in rats with myocardial infarction through the protein kinase B/nuclear factor E2-related factor 2 (Akt/Nrf2) signaling pathway.

MATERIALS AND METHODS: A total of 36 Sprague-Dawley rats were randomly divided into three groups, including sham group (n=12), model group (n=12) and butylphthalide group (n=12). In the sham group, the heart was exposed, and normal saline was intraperitoneally injected after the operation. In the model group, acute myocardial infarction (AMI) model was established, and normal saline was intraperitoneally injected after the operation. In the butylphthalide group, AMI model was established, and butylphthalide was intraperitoneally injected after the operation. After intervention for 4 weeks, the rats were killed, and the samples were collected. The morphology of heart tissues was observed via hematoxylin-eosin (HE) staining. The expression of nicotinamide adenine dinucleotide phosphate oxidase-1 (NOX-1) was detected *via* immunohistochemistry. The protein expressions of phosphorylated Akt (p-Akt) and p-Nrf2 were detected via Western blotting. Moreover, the content of interleukin-1β (IL-1β) and tumor necrosis factor-α (TNF-α) was detected via enzyme-linked immunosorbent assay (ELISA). The messenger ribonucleic acid (mRNA) expression levels of IL-1β, TNF-α and NOX-1 were detected via quantitative Polymerase Chain reaction (qPCR). Furthermore, the apoptosis rate of the cells was detected *via* terminal deoxynucleotidyl transferase-mediated dUTP nick end labeling (TUNEL) assay.

RESULTS: The morphology of heart tissues was significantly damaged in the model group and butylphthalide group compared with the sham group. However, it was significantly improved in the butylphthalide group when compared with the model group. The expression level of NOX-1 increased markedly in the model group and butylphthalide group compared with the sham group ($p<0.05$). However, it was remarkably reduced in the butylphthalide group compared with the model group ($p<0.05$). Meanwhile, the protein expression levels of p-Akt and p-Nrf2 were significantly higher in the model group and butylphthalide group than those of the sham group ($p<0.05$). However, the protein expression levels of p-Akt and p-Nrf2 in the butylphthalide group were remarkably lower than the model group ($p<0.05$). The mRNA expression levels of IL-1β, TNF-α and NOX-1 were markedly higher in the model group and butylphthalide group than those of the sham group ($p<0.05$). However, they remarkably declined in the butylphthalide group compared with the model group ($p<0.05$). In addition, the content of IL-1β and TNF-α increased in the model group and butylphthalide group when compared with the sham group ($p<0.05$). The content of IL-1β and TNF-α in the butylphthalide group was significantly lower than the model group ($p<0.05$). Furthermore, the apoptosis rate was significantly higher in the model group and butylphthalide group than the sham group ($p<0.05$), which was significantly lower in the butylphthalide group than the model group ($p<0.05$).

CONCLUSIONS: Butylphthalide inhibits inflammatory and oxidative stress responses after AMI by regulating the Akt/Nrf2 signaling pathway, thereby inhibiting myocardial apoptosis and benefiting the morphological repair of myocardial tissues.

Key Words:
Acute myocardial infarction (AMI), Akt/Nrf2 signaling pathway, Inflammation, Oxidative stress response.

Introduction

With the changes and influence of social environment, the number of patients with acute myocardial infarction (AMI) is increasing year by year in China, showing a younger trend. According to statistics, there are at least 500,000 new cases of

Corresponding Author: Zheng Zhang, BM; e-mail: 2219896654@qq.com

AMI annually. Meanwhile, middle-aged men (45-60 years old) are still at high-risk of AMI[1,2]. AMI, as an important cardiovascular disease, is the leading cause of death in patients and one of the major causes of deaths in the global population as well. After myocardial infarction (MI), unbalanced remodeling will occur in the autonomic nerve. Eventually, sympathetic nerve remodeling leads to ventricular arrhythmia and sudden cardiac death easily[3]. Therefore, the effective treatment of AMI has always been a research focus worldwide.

Butylphthalide (chemical name: dl-3-n-butylphthalide) is a new anti-cerebral ischemic drug manufactured in China. It is also an artificially-synthesized racemate of L-apigenin[4,5]. Clinically, butylphthalide exhibits an excellent therapeutic effect on ischemic stroke, which can block multiple pathological links caused by ischemic stroke. However, a few reports have investigated the effect of butylphthalide on cardiac function after MI. Oxidative stress and inflammation are recognized as important pathological responses. Both of them play key roles in various nervous system diseases, such as Parkinson's disease and Alzheimer's disease. Studies[6,7] have demonstrated that the protein kinase B/nuclear factor E2-related factor 2 (Akt/Nrf2) signaling pathway plays an important role in the process of resisting oxidative stress and inflammation *in vivo*. Therefore, how to effectively regulate the Akt/Nrf2 signaling pathway may become a new idea for the prevention and treatment of related diseases.

Therefore, the aim of this work was to observe the effects of butylphthalide on oxidative stress and inflammatory response in rats with MI through the Akt/Nrf2 signaling pathway. We aimed to further clarify the therapeutic effect of butylphthalide on AMI and its underlying mechanism, which could benefit its clinical popularization and application.

Materials and Methods

Laboratory Animals and Grouping

A total of 36 Sprague-Dawley male rats weighing (200±10) g were randomly divided into three groups, including the sham group (n=12), the model group (n=12) and the butylphthalide group (n=12). All rats were fed in the Laboratory Animal Center with pure water and adequate food under 12/12 h light/dark cycle. This study was approved by the Laboratory Animal Ethics Committee of Lanzhou University Animal Center.

Main Reagents

Butylphthalide (CSPC, Shijiazhuang, China), anti-nicotinamide adenine dinucleotide phosphate oxidase-1 (NOX-1) antibody (Abcam, Cambridge, MA, USA), anti-phosphorylated Akt (p-Akt) antibody (Abcam, Cambridge, MA, USA), anti-p-Nrf2 antibody (Abcam, Cambridge, MA, USA), hematoxylin-eosin (HE) staining kit (Boster, Wuhan, China), immunohistochemistry kit (Maxim, Fuzhou, China), terminal deoxynucleotidyl transferase-mediated dUTP nick end labeling (TUNEL) kit (Maxim, Fuzhou, China), AceQ quantitative Polymerase Chain Reaction (qPCR) SYBR Green Master Mix Kit (Vazyme, Nanjing, China), HiScript II Q RT SμperMix for qPCR (+gDNA wiper) kit (Vazyme, Nanjing, China), optical microscope (Leica DMI 4000B/DFC425C, Munich, Germany), and fluorescence qPCR instrument (ABI 7500, Foster City, CA, USA).

Methods

Modeling and Treatment in Each Group

After successful anesthesia *via* intraperitoneal injection of 2.5% pentobarbital sodium (30 mg/kg), the rats were fixed on the operating table and depilated. After skin preparation and draping with aseptic towels, electrocardiograph was connected. A tracheal cannula was inserted between the 3rd and 4th cartilage rings, and the ventilator was also connected (tidal volume: 7 mL/kg, and respiratory ratio: 1:1). A 3 cm-long longitudinal left parasternal incision was made. Then, the skin, muscles and fascia were cut in turn. The 3rd and 4th ribs were cut off to fully enlarge the thoracic cavity and expose the heart. Subsequently, the pericardium was carefully cut using ophthalmic forceps, and #0 silk thread was inserted between the left auricle and the arterial cone. Next, the electrocardiogram response in the electrocardiograph was observed. Typical ischemic electrocardiogram manifestation indicated the successful establishment of the AMI model in rats. The skin was sutured layer by layer, and the air in the thoracic cavity was discharged. After the recovery of consciousness, the ventilator was withdrawn, and the rats were kept warm and fed in separate cages.

In the sham group, the thoracic cavity was opened only to expose the heart, and #0 silk thread was not inserted between the left auricle and the arterial cone. Then, the skin was sutured layer by layer, and the rats were fed with normal food and pure water every day. In the model

group, the AMI model was established using the above methods. Meanwhile, the rats were fed with normal food and pure water every day after successful modeling, followed by intraperitoneal injection with normal saline once a day. In the butylphthalide group, the AMI model was established using the above methods as well. Meanwhile, the rats were fed with normal food and pure water every day after successful modeling, followed by intraperitoneal injection with butylphthalide (80 mg/kg) once a day. All rats were executed at 4 weeks after the operation, and the tissue samples were collected.

Sampling

After anesthesia, the abdominal cavity was cut open to expose the abdominal aorta. Subsequently, a blood sample was collected from the abdominal aorta using disposable blood-taking needles. Then, 6 rats in each group were perfused with paraformaldehyde and fixed. After stiffness of limbs in rats, heart tissues were collected and fixed in paraformaldehyde for 48 h. Meanwhile, heart tissues were directly collected from the remaining 6 rats in each group, placed in Eppendorf (EP; Eppendorf, Hamburg, Germany) tubes and stored in an ultra-low temperature refrigerator for subsequent use.

HE Staining

Paraffin-embedded tissues were sliced into 5 μm-thick sections, flattened in warm water at 42°C, picked up and baked to prepare paraffin tissue sections. Then, the sections were routinely deparaffinized with xylene solution, dehydrated with gradient alcohol and stained with hematoxylin dye at room temperature for 10 min. After washing and differentiated in hydrochloric acid alcohol solution for several seconds, the sections were washed again and reacted with eosin dye for 30 s. Finally, the sections were rehydrated with gradient alcohol, followed by moderate color development and sealing.

Immunohistochemistry

Paraffin-embedded tissues were sliced into 5 μm-thick sections, flattened in warm water at 42°C, picked up and baked to be prepared into paraffin tissue sections. Then, the sections were routinely deparaffinized with xylene solution and dehydrated with gradient alcohol. The above sections were soaked in the citric acid buffer and heated repeatedly in microwave 3 times (3 min/time). Subsequently, they were braised for 5 min for full antigen retrieval. After washing, endogenous peroxidase blocker was added dropwise onto sections for 10 min of reaction. The sections were washed again and sealed with goat serum for 20 min. After discarding goat serum, the primary antibody of NOX-1 (1:200) was added for incubation in a refrigerator at 4°C overnight. On the next day, the sections were washed, and reacted with the secondary antibody for 10 min. After fully washing again, they were reacted with a streptavidin-peroxidase solution for 10 min. Finally, color development with diaminobenzidine (DAB; Solarbio, Beijing, China), nucleus counterstaining with hematoxylin, sealing and observation were performed.

Western Blot

Heart tissues stored under ultra-low temperature were added with lysis buffer, followed by an ice bath for 1 h and centrifugation at 14,000 g for 10 min. The concentration of extracted protein was quantified using the bicinchoninic acid (BCA) method (Pierce, Waltham, MA, USA). The absorbance value was detected using a microplate reader, and the standard curves were plotted. Subsequently, extracted protein samples were separated by sodium dodecyl sulphate-polyacrylamide gel electrophoresis (SDS-PAGE). Electrophoresis was terminated when the Marker protein reached the bottom of the glass plate in a straight line. The proteins were then transferred onto polyvinylidene difluoride (PVDF) membranes (Millipore, Billerica, MA, USA). After reacting with blocking buffer for 1.5 h, the membranes were incubated with primary antibodies of anti-p-Akt (1:1,000) and anti-p-Nrf2 (1:1000) overnight. On the next day, the membranes were incubated with the corresponding secondary antibody (1:1,000) at room temperature for 2 h. After washing, the color was fully developed in the dark using the chemiluminescence reagent for 1 min.

Quantitative Polymerase Chain Reaction (qPCR)

Total RNA in heart tissues stored was extracted according to the instructions of RNA extraction reagent. Then, extracted total RNA was reversely transcribed into complementary deoxyribose nucleic acid (cDNA) using the Reverse Transcription kit. The reaction system was 20 μL, and the specific reaction conditions were as follows: reaction at 53°C for 5 min, pre-denaturation at 95°C for 10 min, denaturation at 95°C for 10 s and annealing at 62°C for 30 s, for a total of 35 cycles. The ΔCt

Table I. Primer sequences.

Name	Primer sequence
NOX-1	Forward primer: 5'-TGGCGATGGCAGTGTCTTAG-3' Reverse primer: 5'-GTGCAGGGTCCGAGGT-3'
TNF-α	Forward primer: 5'-TGGCGATGGCAGTGTCTTAG-3' Reverse primer: 5'-GTGCAGGGTCCGAGGT-3'
IL-1β	Forward primer: 5'-TGGCGATGGCAGTGTCTTAG-3' Reverse primer: 5'-GTGCAGGGTCCGAGGT-3'
GAPDH	Forward primer: 5'-ACGGCAAGTTCAACGGCACAG-3' Reverse primer: 5'-GAAGACGCCAGTAGACTCCACGAC-3'

value was first calculated, and the difference in the expression of target genes was calculated. The primer sequences used in this study were shown in Table I.

TUNEL Assay

Paraffin-embedded tissues were sliced into 5 μm-thick sections, flattened in warm water at 42°C, picked up and baked to be prepared into paraffin tissue sections. Then, the sections were routinely deparaffinized with xylene solution and dehydrated with gradient alcohol. TdT reaction solution was added dropwise for reaction in the dark for 1 h. After that, deionized water was added dropwise for 15 min of incubation to terminate the reaction. Subsequently, endogenous peroxidase was inactivated with hydrogen peroxide and the working solution was added dropwise for reaction for 1 h. Finally, the sections were washed, followed by color development with DAB, washing, sealing and observation.

Enzyme-Linked Immunosorbent Assay (ELISA)

Collected heart tissues were first homogenized. The content of inflammatory factors (including IL-1β and TNF-α) was detected according to the instructions of ELISA kits (R&D Systems, Minneapolis, MN, USA).

Statistical Analysis

Statistical Product and Service Solutions (SPSS) 20.0 software (IBM, Armonk, NY, USA) was used for all statistical analysis. *t*-test was used for data in line with normal distribution and homogeneity of variance. A corrected *t*-test was applied for data in line with normal distribution and heterogeneity of variance. A non-parametric test was used for data not in line with normal distribution and homogeneity of variance. One-way ANOVA was conducted to compare the differences among different groups, followed by Post-Hoc Test (Least Significant Difference). Rank sum test was adopted for ranked data, and the chi-square test was adopted for enumeration data. $p< 0.05$ was considered statistically significant.

Results

Morphology of Heart Tissues Via HE Staining

In the sham group, myocardial cells showed no marked morphological abnormality. The structure was complete and regular, and myocardial fibers were arranged orderly. In the model group, myocardial cells exhibited significant damage with irregular morphology, incomplete structure and disordered arrangement. There were rupture and necrosis of myocardial fibers with irregular morphology and incomplete structure. Meanwhile, fibroblast proliferation and scar tissue formation could be observed. In the butylphthalide group, despite the partial loss of myocardial cells, both morphology and structure were remarkably improved compared with those of the model group (Figure 1).

NOX-1 Expression Detected Via Immunohistochemistry

The positive expression of NOX-1 displayed brown color. Immunohistochemistry showed that the positive expression of NOX-1 was significantly down-regulated in the sham group, whereas up-regulated in the model group (Figure 2). According to statistical results (Figure 3), the mean optical density (OD) values of NOX-1 positive expression in the model group and butylphthalide group were significantly increased when compared with the sham group, showing a statistically significant differences ($p<0.05$). Furthermore, the mean OD value of NOX-1

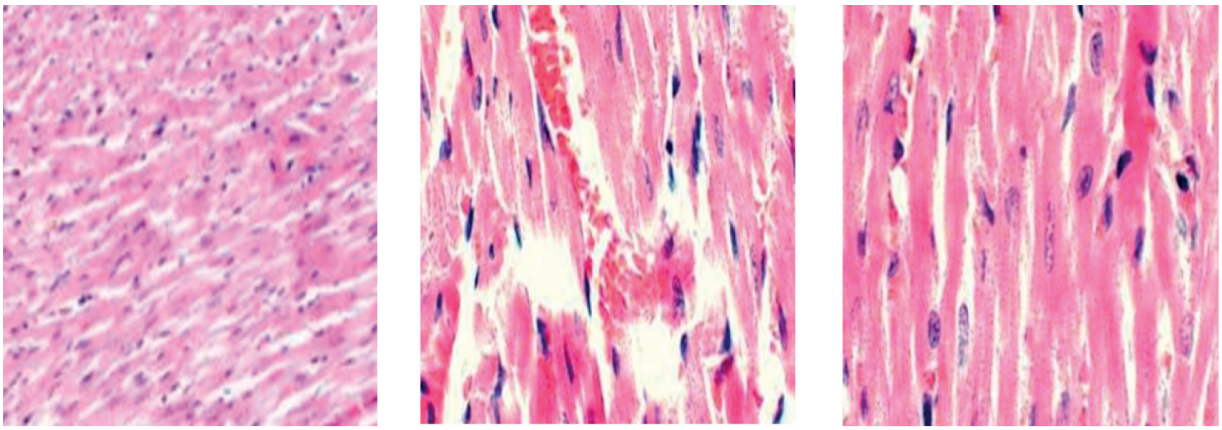

Figure 1. Morphology of heart tissues *via* HE staining (Magnification × 40).

positive expression in the butylphthalide group declined significantly compared with the model group, and the difference was statistically significant ($p<0.05$).

Protein Expression of p-Akt and p-Nrf2 Via Western Blotting

Western blotting results demonstrated that the protein expressions of p-Akt and p-Nrf2 in the sham group were remarkably lower, which was markedly higher in the model group (Figure 4). According to statistical results (Figure 5), the relative protein expression levels of p-Akt and p-Nrf2 increased significantly in the model group when compared with the sham group, showing statistically significant differences ($p<0.05$). However, the expression levels of p-Akt and p-Nrf2 were remarkably reduced in the butylphthalide group when compared with the model group, showing statistically significant differences ($p<0.05$).

The mRNA Expressions of IL-1β, TNF-α and NOX-1 Via qPCR

As shown in Figure 6, the mRNA expression levels of IL-1β, TNF-α and NOX-1 in the model group and butylphthalide group were significantly higher than those of the sham group, displaying statistically significant differences ($p<0.05$). However, the expressions of the three molecules in the butylphthalide group were remarkably lower than the model group ($p<0.05$).

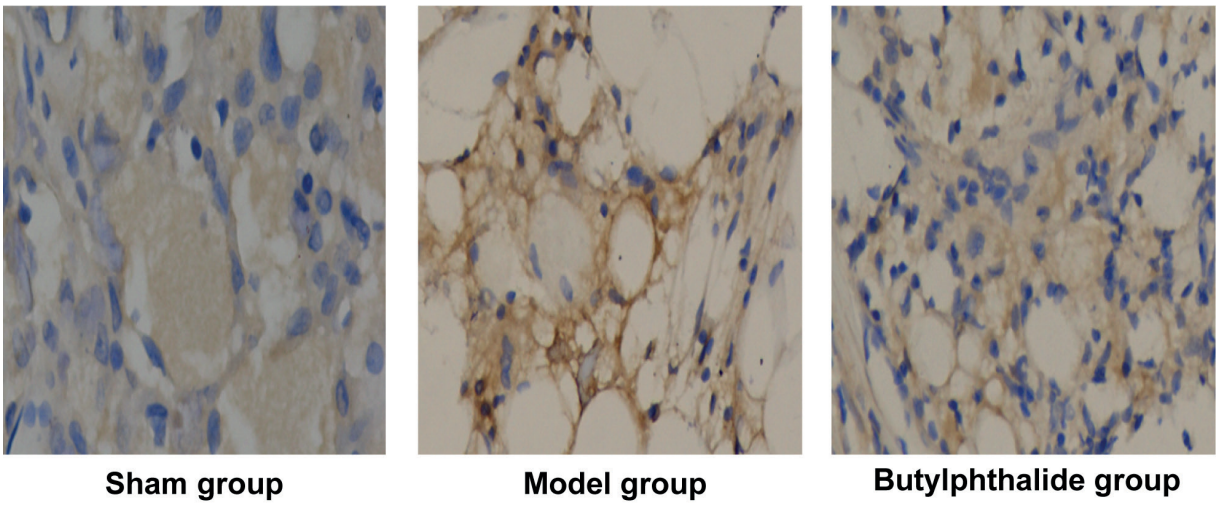

Figure 2. NOX-1 expression detected *via* immunohistochemistry (Magnification × 40).

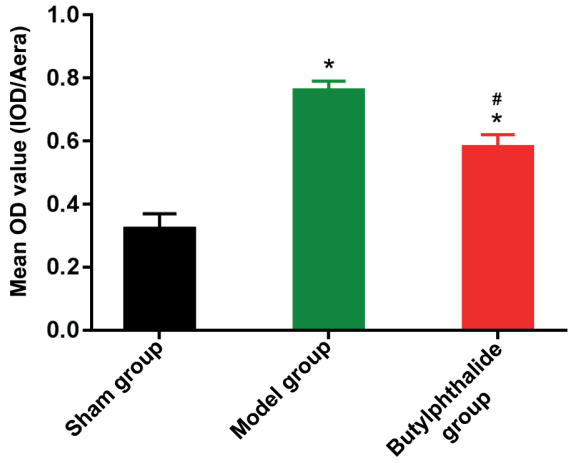

Figure 3. Mean OD value of NOX-1 positive expression in each group. Note: p*<0.05 *vs.* sham group, p#<0.05 *vs.* model group.

Apoptosis Rate Via TUNEL Assay

As shown in Figure 7, the apoptosis rate of the sham group, model group and butylphthalide group was (11.22±5.44)%, (29.36±4.48)% and (16.44±5.21)%, respectively. It could be found that the apoptosis rate in the model group and butylphthalide group was markedly higher than that of the sham group, and the differences were statistically significant (p<0.05). Moreover, the apoptosis rate in the butylphthalide group decreased remarkably compared with the model group, showing statistically significant difference (p<0.05).

Content of IL-1β and TNF-α Via ELISA

As shown in Figure 8, the content of IL-1β and TNF-α in the model group and butylphthalide group was remarkably higher than that of the sham group, showing statistically significant differences (p<0.05). However, the content of IL-1β and TNF-α in the butylphthalide group decreased markedly when compared with the model group (p<0.05).

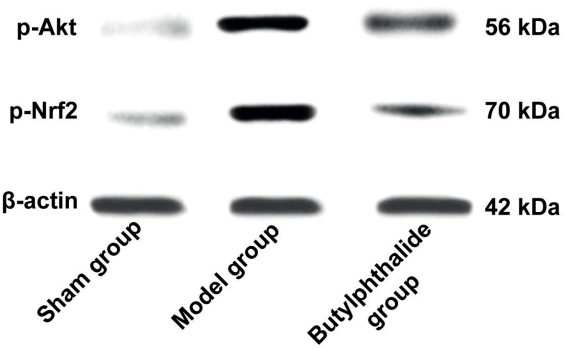

Figure 4. Related protein expressions detected *via* Western blotting.

Discussion

AMI is a common critical disease in the clinic at present. It may often lead to death in patients, making it a major killer of human health[8,9]. The pathological response of AMI is complex, including inflammatory, oxidative stress responses and apoptosis. These complex cellular and molecular mechanisms, as well as a series of complex cascades, often affect ventricular remodeling after AMI. Meanwhile, they play important roles in repair and healing after AMI[10]. Inflammatory and oxidative stress responses are important pathological responses affecting ventricular remodeling after MI. They have close correlations with myocardial apoptosis or necrosis, pathological hypertrophy of myocardial cells and extracellular matrix metabolic disorders[11,12]. Studies[13,14] have demonstrated that after MI, excessive inflammatory and oxidative stress responses can lead to secondary myocardial scar hyperplasia, fibrosis, myocardial apoptosis, etc. Furthermore, they can cause morphological abnormality in tissues and struc-

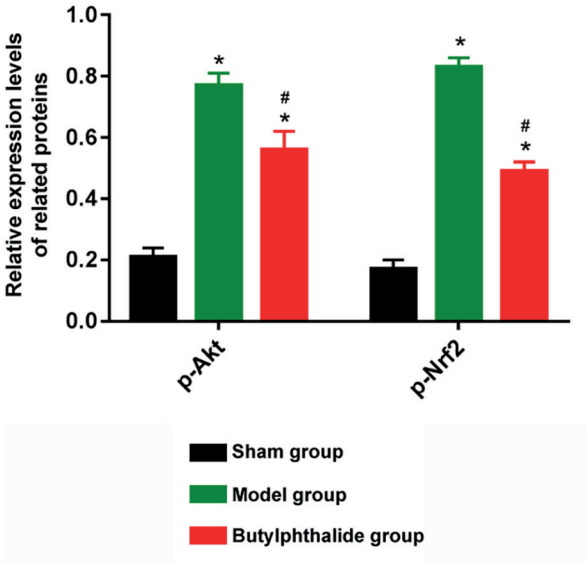

Figure 5. Relative expression levels of proteins in each group. Note: p*<0.05 *vs.* sham group, p#<0.05 *vs.* model group.

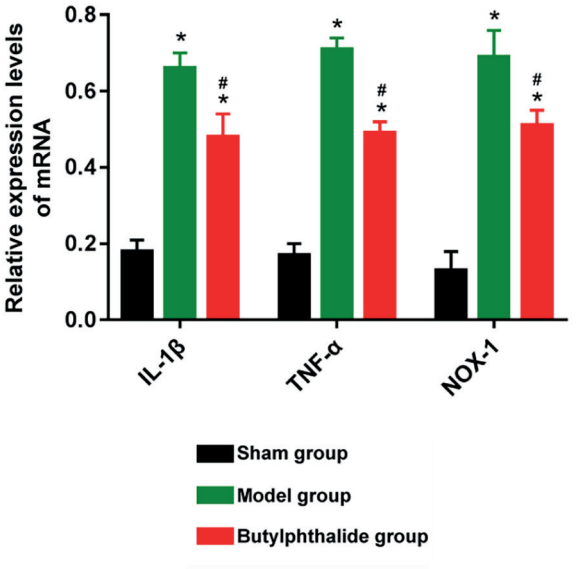

Figure 6. Relative expression levels of mRNAs in each group. Note: p*<0.05 *vs.* sham group, p#<0.05 *vs.* model group.

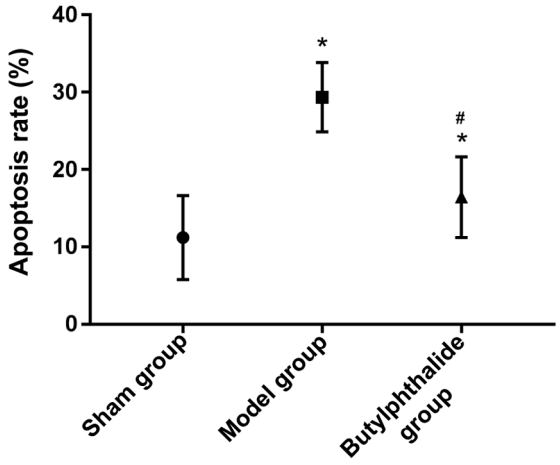

Figure 7. Apoptosis rate in each group. Note: p*<0.05 *vs.* sham group, p#<0.05 *vs.* model group.

ture disorder and dysfunction in the MI region. Ultimately, this results in poor ventricular remodeling and death in severe patients. In addition, how to effectively regulate inflammatory and oxidative stress responses after AMI is of important significance in the treatment of AMI and the improvement of ventricular remodeling after AMI.

As an important cellular signal transduction pathway, Akt/Nrf2 plays an important regulatory role in pathological responses, such as inflammatory and oxidative stress responses. Akt is a kind of important protein kinase B. Its family members include 3 subtypes (type 1, 2 and 3), all of which can be encoded by PKB, activated and phosphorylated. Then, changes can be found in spatial conformation and two amino acid residues are fully exposed. This may initiate the phosphorylation process, exerting an important role in signal transduction[15,16]. Nrf2 is an important member of the transcription factor family. It is considered an important regulator of oxidative stress response as well. Under normal conditions, Nrf2 can be regulated in dependence on Keap1, thereby exerting a negative regulatory effect[17,18]. Under pathological conditions, the normal connection structure between Nrf2 and Keap1 can be destroyed by various stimuli transmitted by the injury. Therefore, Nrf2 is activated and phosphorylated, which enters the nucleus to serve as a transcription factor. After that, it can regulate the expression of cytokines and proteins closely related to oxidative stress and inflammatory responses, participate in oxidative stress and inflammatory responses, and mediate various pathological responses after injury[19,20].

Butylphthalide is a kind of anti-ischemic drug independently developed in China, whose main component is L-apigenin. However, its anti-inflammatory and anti-oxidative stress effects in AMI, as well as the possible underlying mechanism, remain unclear. In the present work, it was found that butylphthalide could effectively inhibit the content of inflammatory factors (IL-1β and TNF-α) and the expression of NOX-1, showing an oxidative stress effect in the MI region after AMI. Meanwhile, it could effectively improve the morphology of tissues in the MI region. Our findings indicated that butylphthalide might benefit the improvement of myocardial tissue morphology by inhibiting inflammatory and oxidative stress responses in the MI region after AMI. Further studies found that butylphthalide effectively suppressed the protein expressions of p-Akt and p-Nrf2 in the MI region after AMI. Moreover, it could effectively reduce the apoptosis rate of MI. The above results all suggested that butylphthalide might exert an important regulatory effect on the Akt/Nrf2 signaling pathway.

Conclusions

Butylphthalide inhibits inflammatory and oxidative stress responses after AMI by regulating

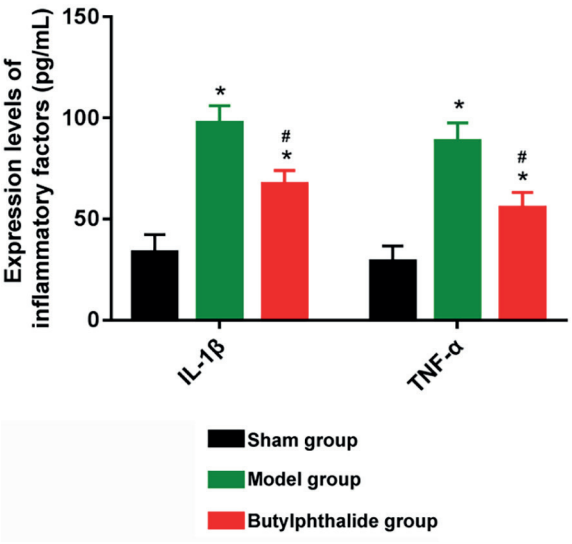

Figure 8. Expression levels of inflammatory factors in each group. Note: p*<0.05 *vs.* sham group, p#<0.05 *vs.* model group.

the Akt/Nrf2 signaling pathway, thereby inhibiting myocardial apoptosis rate and benefiting morphological repair of myocardial tissues.

Conflict of Interests

The Authors declare that they have no conflict of interests.

Funding Acknowledgments

This work was supported by The Natural Science Foundation of Gansu Province (17JR5RA268).

References

1) Sabin P, Koshy AG, Gupta PN, Sanjai PV, Sivaprasad K, Velappan P, Vellikat Velayudhan R. Predictors of no-reflow during primary angioplasty for acute myocardial infarction, from Medical College Hospital, Trivandrum. Indian Heart J 2017; 69: S34-S45.
2) Duyuler PT, Duyuler S, Demir M. Impact of myocardial blush grade on Tpe interval and Tpe/QT ratio after successful primary percutaneous coronary intervention in patients with ST elevation myocardial infarction. Eur Rev Med Pharmacol Sci 2017; 21: 143-149.
3) Noguchi T, Yasuda S, Shibata T, Kawakami S, Tanaka T, Asaumi Y, Kanaya T, Nagai T, Nakao K, Fujino M, Nagatsuka K, Ishibashi-Ueda H, Nishimura K, Miyamoto Y, Kusano K, Anzai T, Goto Y, Ogawa H. Response to letter regarding article, "prevalence, clinical features, and prognosis of acute myocardial infarction attributable to coronary artery embolism". Circulation 2016; 133: e379.
4) Zhang P, Guo ZF, Xu YM, Li YS, Song JG. N-Butylphthalide (NBP) ameliorated cerebral ischemia reperfusion-induced brain injury via HGF-regulated TLR4/NF-kappaB signaling pathway. Biomed Pharmacother 2016; 83: 658-666.
5) Wen XR, Tang M, Qi DS, Huang XJ, Liu HZ, Zhang F, Wu J, Wang YW, Zhang XB, Guo JQ, Wang SL, Liu Y, Wang YL, Song YJ. Butylphthalide suppresses neuronal cells apoptosis and inhibits JNK-caspase3 signaling pathway after brain ischemia/reperfusion in rats. Cell Mol Neurobiol 2016; 36: 1087-1095.
6) Wu J, Li Q, Wang X, Yu S, Li L, Wu X, Chen Y, Zhao J, Zhao Y. Neuroprotection by curcumin in ischemic brain injury involves the Akt/Nrf2 pathway. PLoS One 2013; 8: e59843.
7) Padiya R, Chowdhury D, Borkar R, Srinivas R, Pal BM, Banerjee SK. Garlic attenuates cardiac oxidative stress via activation of PI3K/AKT/Nrf2-Keap1 pathway in fructose-fed diabetic rat. PLoS One 2014; 9: e94228.
8) Phan K, Phan S, Khuong JN, Yan TD. Intra-aortic balloon pump therapy for acute myocardial infarction: Trial sequential analysis. Int J Cardiol 2016; 202: 520-521.
9) Heusch G, Gersh BJ. The pathophysiology of acute myocardial infarction and strategies of protection beyond reperfusion: a continual challenge. Eur Heart J 2017; 38: 774-784.
10) O'Donoghue ML, Glaser R, Cavender MA, Aylward PE, Bonaca MP, Budaj A, Davies RY, Dellborg M, Fox KA, Gutierrez JA, Hamm C, Kiss RG, Kovar F, Kuder JF, Im KA, Lepore JJ, Lopez-Sendon JL, Ophuis TO, Parkhomenko A, Shannon JB, Spinar J, Tanguay JF, Ruda M, Steg PG, Theroux P, Wiviott SD, Laws I, Sabatine MS, Morrow DA. Effect of losmapimod on cardiovascular outcomes in patients hospitalized with acute myocardial infarction: a randomized clinical trial. JAMA 2016; 315: 1591-1599.
11) Minamisawa M, Motoki H, Izawa A, Kashima Y, Hioki H, Abe N, Miura T, Ebisawa S, Miyashita Y, Koyama J, Ikeda U. Comparison of inflammatory biomarkers in outpatients with prior myocardial infarction. Int Heart J 2016; 57: 11-17.
12) Li T, Wei X, Evans CF, Sanchez PG, Li S, Wu ZJ, Griffith BP. Left ventricular unloading after acute myocardial infarction reduces MMP/JNK associated apoptosis and promotes FAK cell-survival signaling. Ann Thorac Surg 2016; 102: 1919-1924.
13) Zhang Y, Li C, Meng H, Guo D, Zhang Q, Lu W, Wang Q, Wang Y, Tu P. BYD ameliorates oxidative stress-induced myocardial apoptosis in heart failure post-acute myocardial infarction via the P38 MAPK-CRYAB signaling pathway. Front Physiol 2018; 9: 505.
14) Chen H, Xu Y, Wang J, Zhao W, Ruan H. Baicalin ameliorates isoproterenol-induced acute myocar-

dial infarction through iNOS, inflammation and oxidative stress in rat. Int J Clin Exp Pathol 2015; 8: 10139-10147.

15) Du X, Xu H, Jiang H, Xie J. Akt/Nrf2 activated upregulation of heme oxygenase-1 involves in the role of Rg1 against ferrous iron-induced neurotoxicity in SK-N-SH cells. Neurotox Res 2013; 24: 71-79.

16) Huang CS, Lin AH, Yang TC, Liu KL, Chen HW, Lii CK. Shikonin inhibits oxidized LDL-induced monocyte adhesion by suppressing NFkappaB activation via up-regulation of PI3K/Akt/Nrf2-dependent antioxidation in EA.hy926 endothelial cells. Biochem Pharmacol 2015; 93: 352-361.

17) Qin X, Qiu C, Zhao L. Maslinic acid protects vascular smooth muscle cells from oxidative stress through Akt/Nrf2/HO-1 pathway. Mol Cell Biochem 2014; 390: 61-67.

18) Cui Q, Li X, Zhu H. Curcumin ameliorates dopaminergic neuronal oxidative damage via activation of the Akt/Nrf2 pathway. Mol Med Rep 2016; 13: 1381-1388.

19) de Oliveira MR, Ferreira GC, Schuck PF, Dal Bosco SM. Role for the PI3K/Akt/Nrf2 signaling pathway in the protective effects of carnosic acid against methylglyoxal-induced neurotoxicity in SH-SY5Y neuroblastoma cells. Chem Biol Interact 2015; 242: 396-406.

20) Lei SW, Cui G, Leung GPH, Luk SCW, Hoi MPM, Wang L, Mahady GB, Lee SMY. Icaritin protects against oxidative stress-induced injury in cardiac H9c2 cells via Akt/Nrf2/HO-1 and calcium signalling pathways. J Funct Foods 2015; 18: 213-223.